American Mineralogist, Volume 83, pages 1176–1181, 1998

High-pressure $P2_1/c$-$C2/c$ phase transitions in clinopyroxenes: Influence of cation size and electronic structure

THILO ARLT,[1,4,*] ROSS J. ANGEL,[2] RONALD MILETICH,[2,5] THOMAS ARMBRUSTER,[3] AND TJERK PETERS[1]

[1]Mineralogisch-Petrographisches Institut, Universität Bern, Baltzerstr.1, CH 3012 Bern, Switzerland
[2]Bayerisches Geoinstitut, Universität Bayreuth, D 95440 Bayreuth, Germany
[3]Laboratorium für Chemische und Mineralogische Kristallographie, Universität Bern, Freiestrasse 3, CH 3012 Bern, Switzerland
[4]Current address: Bayerisches Geoinstitut, Universität Bayreuth, D 95440 Bayreuth, Germany
[5]Current address: Institut für Kristallographie, ETH-Zentrum, Sonneggstrasse 5, CH-8092 Zürich, Switzerland

ABSTRACT

The high-pressure behavior of the clinopyroxenes kanoite $Mn_{0.9}Mg_{1.1}Si_2O_6$, $MnSiO_3$, and $CrMgSi_2O_6$ (all space group $P2_1/c$) was studied by single-crystal X-ray diffraction in a diamond-anvil cell at room temperature. Phase transitions from $P2_1/c$ to $C2/c$ clinopyroxene were found and reversed at 5.06 ± 0.14 GPa for kanoite, 2.905 ± 0.005 GPa in $MnSiO_3$, and 3.60 ± 0.03 GPa in $CrMgSi_2O_6$. The phase transitions are first-order in character and are accompanied by a volume decrease of approximately 2.3%. The structure of high-pressure $C2/c$ kanoite was determined from single-crystal X-ray intensity data collected at 5.20 GPa, and is very similar to that of high-pressure (HP) $C2/c$-ferrosilite. Although the space group $C2/c$ is the same as for the high-temperature (HT) kanoite form, the two phases have significantly different structures. The silicate chains are extremely kinked in HP kanoite while they are almost straight in HT kanoite. Compared with the transition pressure of clinoenstatite-clinoferrosilite, the new data suggest that the effective ionic radii of M1 and M2 cations do not exclusively control the transition pressure and that the HP $C2/c$ clinopyroxenes with Cr^{2+} and Fe^{2+} gain additional stabilization energy from crystal field effects.

INTRODUCTION

Pyroxenes are major components in the Earth's upper mantle. The stability of a $C2/c$ pyroxene polymorph at upper mantle pressures has been recently demonstrated by the combination of phase equilibria studies in the multi-anvil press (e.g., Pacalo and Gasparik 1990; Kanzaki 1991; Woodland and Angel 1997) with room-temperature X-ray diffraction (XRD) studies of clinopyroxene polymorphs in the diamond-anvil pressure cell (Angel et al. 1992; Hugh-Jones et al. 1994). The latter showed that, under compression, the low-clinopyroxene polymorphs of enstatite and ferrosilite (space group $P2_1/c$) undergo phase transitions to high-pressure clinopyroxene polymorphs with space group $C2/c$. In both enstatite ($MgSiO_3$) and ferrosilite ($FeSiO_3$) the transitions are first-order, reversible (although with hysteresis 2.5 GPa in $MgSiO_3$), and displacive in character, but the pressure of the phase transitions are very different, approximately 6.5 GPa in $MgSiO_3$ and 1.7 GPa in $FeSiO_3$. The fact that the transition occurs at lower pressures in Fe^{2+}-bearing pyroxenes than in pure $MgSiO_3$ (Ross and Reynard 1998, unpublished data) implies that solution of Fe into enstatite will act to stabilize the $C2/c$ polymorph. However, the crystal-chemical reasons for this stabilization have remained unclear until now.

The $P2_1/c$ to $C2/c$ symmetry change at high pressure also occurs upon heating clinoenstatite (Iishi and Kitayama 1995), pigeonite (Smyth 1969; Smyth and Burnham 1972), clinoferrosilite (Sueno et al. 1984), and kanoite (Arlt and Armbruster 1997). But careful comparison of the structures of the HT and HP $C2/c$ polymorphs of ferrosilite suggests that they are different phases (Hugh-Jones et al. 1994). Kanoite, $MnMgSi_2O_6$, is of potential interest in this context because its transition temperature is much lower (<250 °C, Arlt and Armbruster 1997) than in the enstatite-ferrosilite clinopyroxenes and it therefore provides an opportunity to study the relationship between the high-temperature and high-pressure $C2/c$ forms at experimentally more tractable conditions.

To provide further insights into the crystal chemical factors influencing the structure and stability of the high-pressure $C2/c$ clinopyroxene phases and their relationship to the high-temperature forms, we have performed a single-crystal high-pressure diffraction study on kanoite, the Cr^{2+}-bearing pyroxene $CrMgSi_2O_6$, and $MnSiO_3$.

* E-mail: thilo.arlt@uni-bayreuth.de

0003–004X/98/1112–1176$05.00

TABLE 2. Atomic coordinates and isotropic displacement parameters for kanoite, $Mn_{0.84}Mg_{1.16}Si_2O_6$

P(GPa)	Site	*x*/a	*y*/b	*z*/c	B_{eq} (Å³)
0.0	M1	0.25065(9)	0.6537(1)	0.2279(2)	0.58(2)
	M2	0.25487(5)	0.02031(6)	0.2269(1)	0.82(1)
	SiA	0.04220(8)	0.34061(9)	0.2806(2)	0.63(1)
	SiB	0.54959(8)	0.83774(9)	0.2358(2)	0.64(1)
	O1A	0.8671(2)	0.3378(2)	0.1725(4)	0.77(3)
	O1B	0.3741(2)	0.8382(2)	0.1312(4)	0.82(3)
	O2A	0.1188(2)	0.5006(2)	0.3237(4)	0.91(3)
	O2B	0.6281(2)	0.9881(2)	0.3715(4)	0.96(3)
	O3A	0.1042(2)	0.2677(2)	0.5875(4)	0.89(4)
	O3B	0.6047(2)	0.7066(2)	0.4751(4)	0.88(3)
5.2	M1	0	0.9064(6)	1/4	1.09(10)
	M2	0	0.2812(4)	1/4	0.85(6)
	Si	0.2945(4)	0.0910(4)	0.2187(6)	0.87(6)
	O1	0.1225(10)	0.0881(9)	0.1409(14)	1.01(13)
	O2	0.3758(10)	0.2427(10)	0.3615(13)	0.97(13)
	O3	0.3488(10)	0.0514(9)	0.9339(15)	1.15(17)

Note: M1 (0.0 GPa): 0.900(5) Mg and 0.100(5) Mn. M2 (0.0 GPa): 0.256(5) Mg and 0.744(5) Mn. M1 (5.2 GPa): 0.836(10) Mg and 0.164(10) Mn. M2 (5.2 GPa): 0.264(10) Mg and 0.736(10) Mn. $B_{eq} = 8/3\pi^2\Sigma_i[\Sigma_j(U_{ij}a_i \cdot a_j \cdot a_i.a_j)]$.

TABLE 3. Selected interatomic distances in Å and angles in ° for synthetic kanoite

	0.0 GPa ($P2_1/c$)		
	A chain	B chain	5.2 GPa ($C2/c$)
Si-O2	1.593(2)	1.595(2)	1.579(10)
Si-O1	1.614(2)	1.618(2)	1.621(9)
Si-O3′	1.647(2)	1.668(2)	1.660(7)
Si-O3	1.663(2)	1.675(2)	1.656(9)
average (4)	1.629(2)	1.639(2)	1.629(9)
M1-O1	2.159(2)	2.190(2)	2 × 2.113(9)
M1-O1′	2.051(2)	2.076(2)	2 × 2.040(8)
M1-O2	2.042(2)	2.057(2)	2 × 2.012(9)
average (6)	2.096(2)		2.055(9)
M2-O1	2.176(2)	2.146(2)	2 × 2.189(8)
M2-O2	2.118(2)	2.054(2)	2 × 2.046(7)
M2-O3	2.361(2)	2.582(2)	2 × 2.374(8)
average (6)	2.240(2)		2.203(8)
O3-O3-O3	166.28(11)	147.09(11)	140.4(7)

EXPERIMENTAL PROCEDURES AND CRYSTALLOGRAPHIC PARAMETERS

Kanoite crystals were synthesized using the flux-growth method described by Skogby (1994). In flux run (R8091) an oxide mixture of 2 (MnO_2):1 (MgO):3.6 (SiO_2) mol% and a nutrient to $Na_2B_4O_7$-flux ratio of 2:1 by weight was used. This charge was heated at 1100 °C, equilibrated for 24 h, cooled to 750 °C at 4 °C/h, and finally quenched to room temperature. The chemical compositions of the products of these experiments were determined with a CAMECA SX50 electron microprobe. Synthetic tephroite, enstatite, and forsterite were used as standards. The operating conditions were 15 kV accelerating potential and 20 nA beam current. The acquired signals were corrected for atomic number, mass-absorption, and secondary fluorescence effects using the CAMECA-PAP version of the Pouchou and Pichoir (1984) procedure. Average compositions of the kanoite crystals (R8091) were $Mn_{0.91}Mg_{1.10}Si_{1.99}O_6$ (cation element compositions ± 0.06). A structure refinement of a flux-grown kanoite crystal (X7, R8091) was performed using intensity data collected at room conditions with a Siemens 3-circle goniometer equipped with a CCD-detector. Data collection and refinement parameters are given in Table 1[1]. The crystal displayed sharp $h + k =$ odd reflections indicative of $P2_1/c$ symmetry and the refined structural parameters are given in Tables 2 and 3. This structure refinement indicates that Mn and Mg are ordered between the M2 and M1 sites yielding the composition $Mn_{0.84}Mg_{1.16}Si_2O_6$. A kanoite crystal, X9, of the same batch but of a composition slightly closer to the end-member formula was selected for the high-pressure study.

[1] For a copy of Table 1, Document AM-98-016, contact the Business Office of the Mineralogical Society of America (see inside front cover of recent issue) for price information. Deposit items may also be available on the *American Mineralogist* web site at http://www.minsocam.org.

The $MnSiO_3$ clinopyroxene was synthesized in the same multi-anvil run that produced the new phase $MnSi_2O_5$ reported by Arlt et al. (1998), and details of the synthesis are provided in that paper. The crystals exhibited relatively broad diffraction profiles, but the $h + k =$ odd reflections indicative of $P2_1/c$ symmetry had the same widths as the $h + k =$ even reflections. The unit-cell parameters matched the ones published for $MnSiO_3$ (Tokonami et al. 1979).

The Cr-containing clinopyroxene was synthesized from oxides by H. St. C. O'Neill using the methods described in Li et al. (1995). Electron microprobe analysis of the sample yielded a composition for the clinopyroxene of $Cr_{1.01}Mg_{0.99}Si_2O_6$. A room pressure single-crystal structure refinement, to be published elsewhere (Angel and O'Neill, in preparation) yielded the site occupancies M1: 0.852(8) Mg + 0.148(8) Cr, M2: 0.155(8)Mg + 0.845(8) Cr for the $P2_1/c$ pyroxene. The diffraction profiles from the crystal were sharp, and $h + k =$ odd reflections were present.

High-pressure XRD data were collected from kanoite (X9 from run R8091), $MnSiO_3$ and $CrMgSi_2O_6$ single-crystals loaded in turn into a diamond-anvil cell designed by Allan et al. (1996) with 4:1 methanol:ethanol mixture as hydrostatic pressure medium. Unit-cell parameters of the clinopyroxenes were determined at high pressure by the method of eight-position diffracted-beam centering (King and Finger 1979) on a Huber 4-circle diffractometer. Details are given by Angel et al. (1997). For the kanoite experiments, the pressure was determined to a precision of typically 0.01 GPa and an accuracy of 0.025 GPa from the shift of the fluorescence line of a ruby included within the cell, using the calibration of Mao et al. (1986). For the other experiments, pressure was determined from the unit-cell volume of a quartz crystal included in the diamond-anvil cell, using the equation of state of quartz (Angel et al. 1997). Results are presented in Table 4. Because the purpose of these experiments was to locate the $P2_1/c$ to $C2/c$ transition in each sample it was only necessary at some pressures to confirm which phase was present, together with the approximate pres-

TABLE 4. Clinopyroxene unit cell parameters

Experiment	P(GPa)	Type*	*a* (Å)	*b* (Å)	*c* (Å)	β (°)	*V* (Å³)	Space group
				Kanoite				
X9P1†	4.00	R						$P2_1/c$
X9P2†	4.91	R	9.574(4)	8.749(11)	5.174(2)	107.91(6)	412.4(2)	$P2_1/c$
X9P3	5.20‡	R	9.4199(5)	8.7830(4)	5.0201(3)	103.050(5)	404.61(4)	$C2/c$
X9P4	5.05	R						$C2/c$
X9P5	4.93	R	9.5827(4)	8.7622(3)	5.1755(2)	107.760(4)	413.85(3)	$P2_1/c$
X9P6	5.12	R						$P2_1/c$
X9P7	5.20	R	9.4218(4)	8.7861(5)	5.0207(3)	103.071(4)	404.85(3)	$C2/c$
X9P8	0.00	R	9.7196(2)	8.9172(2)	5.2465(2)	108.505(2)	431.21(2)	$P2_1/c$
				$MnSiO_3$				
X8P0	0.00	—	9.866(3)	9.1777(8)	5.3019(11)	108.30(3)	455.8(2)	$P2_1/c$
X8P1	1.403(5)	Q	9.8101(19)	9.1209(5)	5.2672(8)	107.76(2)	448.85(14)	$P2_1/c$
X8P2	3.154(6)	Q	9.613(3)	9.0871(7)	5.0615(11)	102.69(3)	431.36(19)	$C2/c$
X8P3	2.894(5)	Q	9.765(3)	9.0662(9)	5.2407(11)	107.43(3)	442.7(2)	$P2_1/c$
X8P4p§	2.905(5)	Q	9.765(7)	9.075(3)	5.236(4)	107.44(8)	442.7(6)	$P2_1/c$
X8P4c§	2.905(5)	Q	9.629(5)	9.0902(15)	5.069(2)	102.75(6)	432.7(4)	$C2/c$
X8P5	2.916(5)	Q	9.623(2)	9.0951(6)	5.0663(9)	102.75(3)	432.48(15)	$C2/c$
				$CrMgSi_2O_6$				
CrenP0	0.00	—	9.7737(9)	8.9540(10)	5.2624(5)	109.998(6)	432.77(5)	$P2_1/c$
CrenP1	2.740(7)	Q	9.6664(10)	8.8809(12)	5.2147(7)	109.46(1)	422.10(7)	$P2_1/c$
CrenP2	4.756(8)	Q	9.4405(10)	8.8035(12)	5.0297(7)	104.115(9)	405.40(8)	$C2/c$
CrenP3	2.1	T						$P2_1/c$
CrenP4	3.5	T						$P2_1/c$
CrenP5	4.147(8)	Q	9.4583(7)	8.8160(10)	5.0398(4)	104.276(6)	407.26(04)	$C2/c$
CrenP6	3.9	T						$C2/c$
CrenP7	3.7	T						$C2/c$
CrenP8	3.581(8)	Q	9.6361(5)	8.8565(6)	5.2015(3)	109.279(3)	419.02(3)	$P2_1/c$
CrenP9	3.643(7)	Q	9.4713(9)	8.8284(12)	5.0500(5)	104.436(7)	408.93(6)	$C2/c$
CrenP10	8.769(12)	Q	9.3593(10)	8.7166(14)	4.9835(5)	103.561(8)	305.22(6)	$C2/c$

* Measurement on CAD4 diffractometer (all others were HUBER).
† Pressure measurement method; R: ruby, Q: unit-cell volume of quartz, T: subset of quartz reflections (esd ~0.05 GPa).
‡ Data collection for structure refinement of high pressure kanoite.
§ Two coexisting phases.

sure. This was achieved by centering a subset of reflections of the clinopyroxene and, in the case of the $MnSiO_3$ and $CrMgSi_2O_6$ experiments, a subset of the quartz reflections. Although this procedure unambiguously determines the clinopyroxene phase present through the value of the β unit-cell angle of the clinopyroxene, the unit-cell parameters are necessarily less precise than those of a full determination and are therefore not reported in Table 4.

Intensity data were collected on a CAD4 diffractometer (monochromatic Mo radiation) on one synthetic kanoite crystal (X9, R8091) in the *C*2/*c* phase at approximately 5.20 GPa. Data collection procedures are the same as described by Miletich et al. (1997). The ω-scan profiles were inspected visually and then integrated to yield intensity data. Examination of an initial data set collected to $2\theta = 60°$ revealed no significant intensity at the positions of reflections with $h + k = 2n + 1$, or l = odd in *h*0*l*, indicating *C*2/*c* or *Cc* as the possible space groups, the former being confirmed by subsequent successful structure refinement. A second data set was collected including all reflections allowed by *C*2/*c* symmetry, and this was used for structure analysis. After correction for absorption by the crystal ($\mu = 35.4$ cm^{-1}, transmission factors = 0.85–0.87) and the DAC (transmission factors = 0.33–0.39) the data were reduced to structure factors and averaged in Laue group 2/m. The internal agreement index was $R_{int} = 0.035$ for 166 averaged reflections with $I > 3\sigma_I$. Structure refinement proceeded from a starting model based upon the high-pressure *C*2/*c* structure of $FeSiO_3$ clinopyroxene, and converged to $R_u = 0.043$, $R_w = 0.046$, $G_{fit} = 1.4$ for 166 observed reflections and 22 variables (including isotropic displacement parameters for all atoms, and a variable describing the Mg/Mn distribution between the M1 and M2 sites subject to the constraint of the composition determined by microprobe analysis). Refined atom coordinates and the isotropic displacement parameters are reported in Table 2, selected bond-lengths and angles in Table 3.

RESULTS

On increasing pressure to 4.91(1) GPa the kanoite crystal X9 remained in the $P2_1/c$ phase, but transformed to the *C*2/*c* phase on further increase of the pressure to 5.20(1) GPa at which point the data collection for the single-crystal structure refinement was performed. Pressure release to 5.05(1) GPa (*C*2/*c*) and further down to 4.93(1) GPa yielded the expected reversible transformation to the low-form indicated by the reappearance of the *C*2/*c*-forbidden reflections with $h + k = 2n + 1$ and the large value of β. A second cycle through the transition yielded consistent results (Table 4), and a reversed bracket in pressure between 4.93(1) GPa and 5.20(1) GPa with the minimum width of the hysteresis loop being 0.07 GPa [between 5.05(1) and 5.12(1) GPa].

In several cycles (see Table 4), the $P2_1/c$ to HP *C*2/*c* phase transition was reversed between 3.581(8) GPa and

3.643(7) GPa in $CrMgSi_2O_6$, without any detectable hysteresis. In end-member $MnSiO_3$ the transition was initially reversed between 3.154(6) GPa (increasing pressure) and 2.894(5) GPa (decreasing pressure). Upon a subsequent small pressure increase to 2.905(5) GPa diffraction maxima from both the $P2_1/c$ and $C2/c$ phases were found, indicating that the two phases were co-existing within the same ''crystal.'' Even though the intensities of the non-overlapped reflections of each phase were approximately 50% of the intensities found in the single-phase regimes, the cell parameters of both phases could be measured simultaneously. Because chemical inhomogeneities of the synthetic end-member $MnSiO_3$ are unlikely, the effect of pressure-buffering in the diamond-anvil cell is believed to cause this coexistence and allows the transition pressure to be quoted as 2.905(5) GPa.

Discussion

*C*2/*c* structures of kanoite

All pyroxene polymorphs consist of chains of corner-sharing silicate tetrahedra that crosslink, by shared O atoms, parallel bands of octahedrally coordinated cations. The refined site occupancies of the M1 and M2 sites of high-pressure *C*2/*c* kanoite (Table 2), which represent the synthesis condition of above 750 °C at 1 atm, correspond to effective ionic radii of $r(M1) = 0.745$ Å and $r(M2) = 0.795$ Å interpolated from the values of Mg^{2+} (0.72 Å) and Mn^{2+} (0.82 Å) in octahedral coordination (Shannon 1976). These values compare to that of 0.78 Å for octahedrally coordinated Fe^{2+}. Therefore, as expected, the average M1-O bond length (Table 3) in kanoite is intermediate between that found in HP *C*2/*c* ferrosilite (2.14 Å; Hugh-Jones et al. 1994) and in HP *C*2/*c* enstatite (2.02 Å; Angel et al. 1992), and the average M2-O bond length in HP *C*2/*c* kanoite is slightly greater than the 2.18 Å in HP *C*2/*c* ferrosilite leading to a larger volume (13.88 $Å^3$) of the MnO_6 octahedra compared with FeO_6. However, the distortion of the M2 site of HP kanoite (angle variance AV = 55.2; quadratic elongation QE = 1.0219; Robinson et al. 1971) is significantly greater than that in HP ferrosilite, reflecting the different influences of the electronic states of the Mn^{2+} and Fe^{2+} cations. Because the configurations of the cation sites in pyroxenes are intimately related to the configuration of the tetrahedral chains, the overall topology of the high-pressure kanoite structure is very similar to that of ferrosilite. In HP *C*2/*c* kanoite these tetrahedral chains are O-rotated (following Thompson 1970) and strongly kinked with a chain extension angle, O3-O3′-O3″, of 140.4°, similar to the angle in HP *C*2/*c* ferrosilite (138.4°).

The relatively low temperature of the $P2_1/c$ to $C2/c$ transition in kanoite (240 °C, Arlt and Armbruster 1997) allows detailed comparison of the structures of a HT clinopyroxene with a HP clinopyroxene (both *C*2/*c*) at much closer conditions than was previously possible (Hugh-Jones et al. 1994) for $FeSiO_3$ in which the HT phase only appears above 1050 °C (Sueno et al. 1984). Note that the high-temperature study of kanoite by Arlt and Armbruster (1997) only extended to 270 °C, so that structural change due to cation redistribution during the heat treatment can be excluded. However the structural parameters of synthetic kanoite (Table 2 and 3) differ significantly from natural kanoite reported in Gnos et al. (1996) at room temperature. The M1-O bond length of the synthetic sample is larger than in natural kanoite because M1 is almost purely occupied by Mg in the latter, whereas the M2-O bond length is shorter as a result of the synthetic material being Ca-free.

Table 5. Changes in parameters during the $P2_1/c$ to HP $C2/c$ phase transition in clinopyroxenes

Cpx	Δ*a* (%)	Δ*b* (%)	Δ*c* (%)	Δβ (°)	Δ*V* (%)
Kanoite	−1.7	−0.2	−3.0	−4.7	−2.2
$MnSiO_3$	−1.4	0.2	−3.2	−4.7	−2.3
$CrMgSi_2O_6$	−1.7	−0.2	−2.9	−4.8	−2.4
$MgSiO_3$*	−2.1	−0.2	−3.7	−6.1	−2.8
$FeSiO_3$†	−2.3	−0.2	−3.3	−5.0	−2.7

* Angel and Hugh-Jones (1994).
† Hugh-Jones et al. (1994).

In general, the metrical changes due to the high temperature and high pressure phase transitions from $P2_1/c$ to $C2/c$ are similar, but opposite in sign. The changes at high temperature are smaller; in kanoite, the angle β increases only 0.4° to 109.26° in the high temperature transition, and the changes of *a*, *b*, *c*, and *V* are +0.3%, −0.1%, +0.4%, and +0.5%, respectively (Arlt and Armbruster 1997, compare with Table 5 and Fig. 1). Because the unit-cell dimension *b* changes by only 0.2% at the $P2_1/c$ to HP $C2/c$ phase transition, the metrical changes correspond to almost purely a shear of the unit cell in the (010) plane. The same pattern has been observed at the HP phase transitions in $MgSiO_3$ and $FeSiO_3$ (Angel and Hugh-Jones 1994; Hugh-Jones et al. 1994). Generally the changes in kanoite, $MnSiO_3$, and $CrMgSi_2O_6$ are slightly smaller than those observed for $MgSiO_3$ and $FeSiO_3$ (Table 5).

The most significant structural difference between the HT and HP *C*2/*c* structures is the O3-O3′-O3″ tetrahedral chain extension angle (Fig. 2). In high-temperature kanoite (Arlt and Armbruster 1997, at 270 °C) the chain is almost straight with O3-O3-O3 = 175.4°, whereas that of the HP form is extremely kinked (140.4°: Table 3). As for ferrosilite, the configuration of the tetrahedral chain in the HT structure is very similar to the A-chain of $P2_1/c$ kanoite (O3-O3-O3 = 171.7(2)° at 25 °C; Gnos et al. 1996) while the chain extension angle of HP kanoite is close to the B chain extension angle of the $P2_1/c$ phase (147.09(11)° at 25 °C, Table 3). Because the chains run parallel to the *c* axis, these changes in extension angle lead to the large differences in the *c* unit-cell dimension that we noted above. Also, because the tetrahedral chain of the HP *C*2/*c* structure is much more kinked than in the HT structure, both the M1 and M2 sites (⟨M1-O⟩ = 2.089

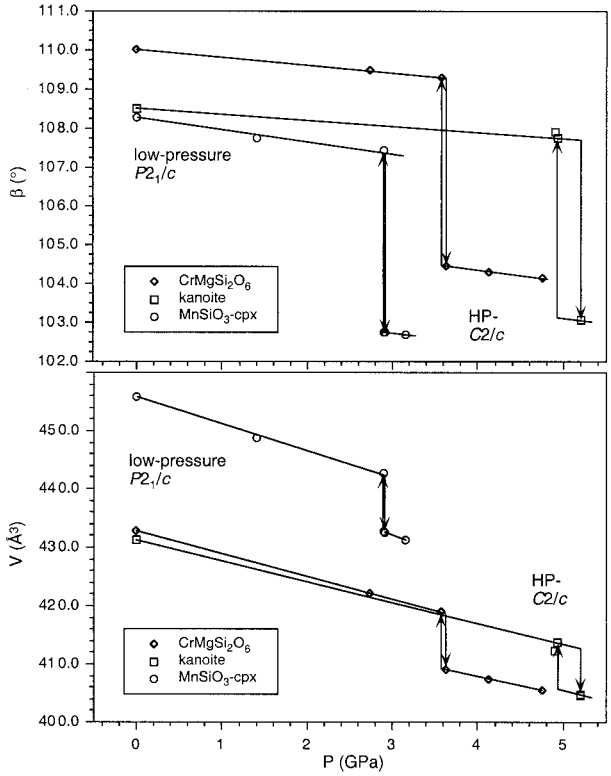

FIGURE 1. The variation of the unit-cell angle β and unit-cell volume with pressure in kanoite (squares), $MnSiO_3$ (circles), and $CrMgSi_2O_6$ (diamonds). The $P2_1/c$ to HP $C2/c$ phase transition is indicated by a strong decrease of β and V at 5.06 ± 0.14 GPa (kanoite), 2.905(5) ($MnSiO_3$) and at 3.60 ± 0.03 GPa ($CrMgSi_2O_6$).

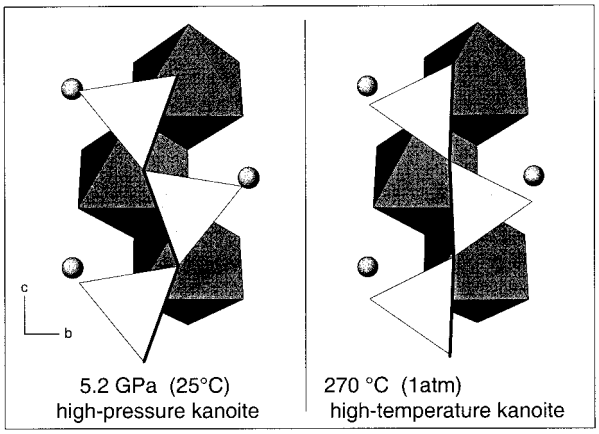

FIGURE 2. Polyhedral representation of the SiO_4-tetrahedral chains in high-temperature $C2/c$ kanoite (Arlt and Armbruster 1997) and in high-pressure $C2/c$ kanoite (this study). HP $C2/c$ phases have extremely kinked tetrahedral chains whereas HT $C2/c$ structures have extended chains.

Å and ⟨M2-O⟩ = 2.289 Å) are larger and more distorted in the HT phase compared to the HP structure.

The differences between the HT and HP $C2/c$ structures, and in particular in the chain extension angles, are much larger than any changes that have been reported to occur as continuous changes in a clinopyroxene as a result of changes in P and/or T without phase transitions. Our new data on HP kanoite therefore support the idea that the HT $C2/c$ and HP $C2/c$ clinopyroxene structures are distinct phases separated by an isosymmetric phase transition or crossover (Christy and Angel 1995). This idea can be tested through in-situ high-pressure, high-temperature diffractometry of kanoite (Arlt et al., in preparation).

Controls on the transition pressure

Determination of the pressures of the $P2_1/c$-$C2/c$ transformation in kanoite, $MnSiO_3$, and $CrMgSi_2O_6$ provides a stringent test of any proposed relationship between the transition pressure and crystal chemistry of clinopyroxenes. Prior to this study, the available data along the $MgSiO_3$-$FeSiO_3$ join (Angel et al. 1992; Hugh-Jones et al. 1994; Ross and Reynard 1998, unpublished data) were consistent with the idea that the transition pressure is a single, smooth function of average cation radius (Fig. 3, open squares). Whereas the 3.60 ± 0.03 GPa pressure for the transition in $CrMgSi_2O_6$ falls approximately on this trend, the transition pressures for the two manganese-containing pyroxenes do not. The discrepancy is exaggerated if the radius of the M2 cation is used as the ordinate in Figure 3; the data points for kanoite and $CrMgSi_2O_6$ then being shifted to the right. Because both Fe^{2+} ($3d^6$) and Cr^{2+} ($3d^4$) possess four unpaired electrons, our results suggest that electronic effects might be an additional in-

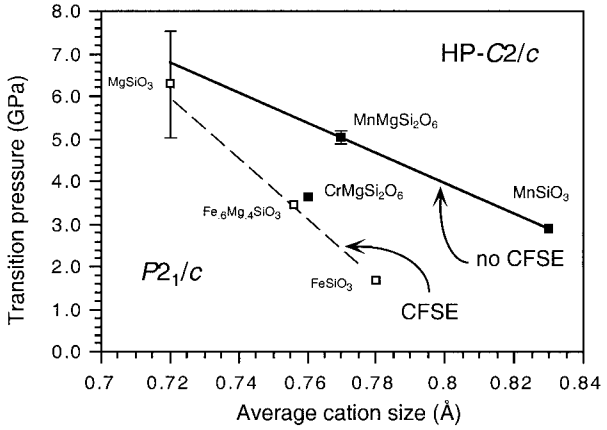

FIGURE 3. Transition pressures of the $P2_1/c$ to HP $C2/c$ transformation in clinopyroxenes plotted as a function of average cation radius. Error bars (only given if larger than symbol size) represent observed hysteresis loops. Transition pressures for $MgSiO_3$ and $FeSiO_3$ are taken from Angel et al. (1992) and Hugh-Jones et al. (1994), respectively, those of intermediate members of the $(Fe,Mg)SiO_3$ series are taken from Ross and Reynard (1998, unpublished data) and are represented by a dashed line. Note that the transition pressure of clinopyroxenes containing Fe^{2+} or Cr^{2+} (crystal field stabilized ions) appear to be shifted to lower pressures.

fluence on the pressure of the $P2_1/c$ to HP $C2/c$ phase transition with a contribution from crystal field effects stabilizing the HP $C2/c$ clinopyroxenes with Cr^{2+} and Fe^{2+}.

A similar reduction of transition pressures occurs for the high-pressure olivine to spinel transformation in Fe_2SiO_4, Co_2SiO_4, and Ni_2SiO_4 (3–7 GPa) compared to Zn_2SiO_4 and Mg_2SiO_4 (13 and 12 GPa) (Syono et al. 1971). This behavior was attributed to excess crystal field stabilization energy (CFSE) for Fe^{2+}, Co^{2+}, and Ni^{2+} in the octahedral sites in spinel over those in olivine (Burns and Sung 1978); their arguments can be transferred to the case of the pyroxenes. For Cr^{2+}- and Fe^{2+}-containing clinopyroxenes there will be an additional contribution to the free energy change associated with the $P2_1/c$ to $C2/c$ transition due to the different CFSE for these ions in the octahedral sites in the two phases. This energy contribution, ΔG_{CFS} consists of an enthalpy term ΔH_{CFS} and an entropy term $T\Delta S_{CFS}$ (e.g., Burns 1993). The sign of the enthalpy term will be determined by a balance between a negative contribution (i.e., greater CFSE) because the octahedral sites in the HP $C2/c$ polymorph are significantly smaller than those in the $P2_1/c$ structure ($\Delta \alpha R^{-5}$), and a positive term arising from the fact that the M2 sites in the $C2/c$ structure are less distorted than those in the $P2_1/c$ structure. The decrease in distortion will, however, also give rise to a counterbalancing positive ΔS_{CFS} term arising from an increase in electronic entropy. Because we observe a stabilization of the $C2/c$ form by $Cr^{2+}$and Fe^{2+} we conclude that the volume decrease of the octahedral sites is the dominant factor and leads to a negative sign of ΔG_{CFS}.

Acknowledgments

Reviews by J.R. Smyth, D.C. Palmer, and N.L. Ross helped improve the manuscript. The synthesis of $MnSiO_3$ was performed with P. Ulmer at the ETH-Zurich, Switzerland, and the $CrMgSi_2O_6$ was synthesized by H. St. C. O'Neill at A.N.U., Canberra. T. Arlt is indebted to the Schweizerischer Nationalfonds for financial support (Credit 20-33562.92 to T. Peters). X-ray diffraction experiments at the Bayerisches Geoinstitut were performed with the support of the EC ''Human and Capital Mobility—Access to Large Scale Facilities'' program (Contract no. ERBCHGECT940053 to D. Rubie). Support is acknowledged for the electron microprobe at the University of Bern by Schweizerischer Nationalfonds (Credit 21-26579.89).

Refrences cited

Allan, D.R., Miletich, R., and Angel, R.J. (1996) A diamond-anvil cell for single-crystal X-ray diffraction studies to pressures in excess of 10 GPa. Reviews of Scientific Instruments, 67, 840–842.

Akimoto, S. and Syono, Y. (1972) High pressure transformations in $MnSiO_3$. American Mineralogist, 57, 76–84.

Angel, R.J. and Hugh-Jones, D.A. (1994) Equations of state and thermodynamic properties of enstatite pyroxenes. Journal of Geophysical Research, 99, 19777–19783.

Angel, R.J., Chopelas, A., and Ross, N.L. (1992) Stability of high-density clinoenstatite at upper-mantle pressures. Nature, 358, 322–324.

Angel, R.J., Allan, D.R., Miletich, R., and Finger, L.W. (1997) The use of quartz as an internal pressure standard in high-pressure crystallography. Journal of Applied Crystallography, 30, 461–466.

Arlt, T. and Armbruster, T. (1997) The temperature dependent $P2_1/c$-$C2/c$ phase transition in the clinopyroxene kanoite $MnMg[Si_2O_6]$: a single-crystal X-ray and optical study. European Journal of Mineralogy, 9, 953–964.

Arlt, T., Armbruster, T., Ulmer, P., and Peters, T. (1998) $MnSi_2O_5$ with the titanite structure: A new high-pressure phase in the MnO-SiO_2 binary. American Mineralogist, 83, 657–660.

Burns, R.G. (1993) Mineralogical Applications of Crystal Field Theory (Second Edition), 551 p. Cambridge University Press, U.K.

Burns, R.G. and Sung, C.M. (1978) The effect of crystal field stabilization on the olivine → spinel transition in the system Mg_2SiO_4-Fe_2SiO_4. Physics and Chemistry of Minerals, 2, 349–364.

Christy, A. and Angel, R.J. (1995) A model for the origin of the cell-doubling phase transition in clinopyroxene and body-centred anorthite. Physics and Chemistry of Minerals, 22, 129–135.

Gnos, E., Armbruster, T., and Nyfeler, D. (1996) Kanoite, donpeacorite and tirodite: Mn-Mg-silicates from a manganiferous quartzite in the United Arab Emirates. European Journal of Mineralogy, 8, 251–261.

Hugh-Jones, D., Woodland, A., and Angel, R. (1994) The structure of high-pressure $C2/c$ ferrosilite and crystal chemistry of high-pressure $C2/c$ pyroxenes. American Mineralogist, 79, 1032–1041.

Iishi, K. and Kitayama, K. (1995) Stability of high clinoenstatite. Neues Jahrbuch Mineralogische Monatshefte, 1995(2), 65–74.

Kanzaki, M. (1991) Ortho/clinoenstatite transition. Physics and Chemistry of Minerals, 17, 726–730.

King, H. and Finger, L.W. (1979) Diffracted beam crystal centering and its application to high-pressure crystallography. Journal of Applied Crystallography, 12, 374–378.

Li, J.-P., O'Neill, H.St.C., and Seifert, S. (1995) Subsolidus phase equilibria in the system MgO-SiO_2-Cr-O in equilibrium with metallic Cr, and their significance for the petrochemistry of chromium. Journal of Petrology, 36, 107–132.

Mao, H.K., Xu, J., and Bell, P.M. (1986) Calibration of the ruby pressure gauge to 800 kbar under quasi-hydrostatic conditions. Journal of Geophysical Research, 91, 4673–4676.

Miletich, R., Allan, D.R., and Angel, R.J. (1997) Structural control of polyhedral compression in synthetic braunite, $Mn^{2+}Mn^{3+}{}_6O_8SiO_4$. Physics and Chemistry of Minerals, 25, 183–192.

Pacalo, R.E.G. and Gasparik, T. (1990) Reversals of the orthoenstatite-clinoenstatite transition at high pressures and high temperatures. Journal of Geophysical Research, 95, 15853–15858.

Pouchou, J.L. and Pichoir, F. (1984) Un nouveau modèle de calcul pour la microanalyse quantitative par spectrométrie de rayons X. La Recherche Aérospatiale, 3, 167–192.

Robinson, K., Gibbs, G.V., and Ribbe, P.H. (1971) Quadratic elongation: A quantitative measure of distortion in coordination polyhedra. Science, 172, 567–570.

Shannon, R.D. (1976) Revised effective ionic radii and systematic studies of interatomic distances in halides and chalcogenides. Acta Crystallographica, A32, 751–767.

Skogby, H. (1994) OH incorporation in synthetic clinopyroxene. American Mineralogist, 79, 240–249.

Smyth, J.R. (1969) Orthopyroxene-high-low-clinopyroxene inversions. Earth and Planetary Science Letters, 6, 406–407.

Smyth, J.R. and Burnham, C.W. (1972) The crystal structures of high and low clinohypersthene. Earth and Planetary Science Letters, 14, 183–189.

Sueno, S., Kimata, M., and Prewitt, C.W. (1984) The crystal structure of high clinoferrosilite. American Mineralogist, 69, 264–269.

Syono, Y., Tokonami, M., and Matsui, Y (1971) Crystal field effect on the olivine-spinel transformation. Physics of the Earth and Planetary Interiors, 4, 347–352.

Thompson, J.B. Jr. (1970) Geometrical possibilities for amphibole structures: Model biopyriboles. American Mineralogist, 55, 292–293.

Tokonami, M., Horiuchi, H., Nakano, A., Akimoto, S., and Morimoto, N. (1979) The crystal structure of the pyroxene-type $MnSiO_3$. Mineralogical Journal, 9, 424–426.

Woodland, A.B. and Angel, R.J. (1997) Reversal of the orthoferrosilite-high-P clinoferrosilite transition, a phase diagram for $FeSiO_3$ and implications for the mineralogy of the Earth's upper mantle. European Journal of Mineralogy, 9, 245–254.

Manuscript received December 19, 1997
Manuscript accepted July 14, 1998
Paper handled by Nancy L. Ross